The EPR signal for the S_2 state of PS II is really a difference spectrum between those for PS II in the S_2 state and PS II in the S_1 state.[7,8] Such S_2-state EPR spectra were determined at different frequencies by Hansson et al.[51] They found that the 18-20 manganese hyperfine lines on the $g \cong 2$ signal observed at 9.4 GHz did not separate into identifiable hyperfine-structured g_x, g_y, or g_z signals at 36 GHz. It could be concluded that the **g**-tensor anisotropy is too small to be seen at 34 GHz. Alternatively, it is possible that at both X- and Q-band frequencies the manganese hyperfine structure on only one of the **g**-tensor components of the $S = {}^1/_2$ state is seen. Distributions in environments about the polymanganese S_2 state in the chloroplast could lead to strain effects.

Several $Mn^{III}Mn^{IV}$ complexes such as $[(bipy)_2Mn<^{O}_{O}>Mn(bipy)_2]^{3+}$ have been shown[32-34] to give in a glass medium $g \cong 2$ EPR signals which are structured with 16 manganese hyperfine lines. These $Mn^{III}Mn^{IV}$ complexes exhibit antiferromagnetic interactions with exchange parameters in the range $J = -40$ to -220 cm^{-1}. All simulations of these spectra have been performed by assuming an isotropic **g** tensor for the $S = {}^1/_2$ ground state, together with isotropic hyperfine **A** tensors for the Mn^{III} and Mn^{IV} ions. Very recently, the EPR spectrum reported[32b] for a *polycrystalline* sample of a $Mn^{III}Mn^{IV}$ complexes was also found to exhibit a 16-line manganese hyperfine pattern. Careful examination of the simulated and experimental EPR spectra for these $Mn^{III}Mn^{IV}$ complexes shows that the simulations are not very good. Only some signals at low field and at high field are simulated well. However, the relative intensities and line shapes are in many cases quite different between the simulated and experimental spectra. This is particularly true for the hyperfine-structured $g \cong 2$ signal seen[32b] for the polycrystalline sample of $[L_2Mn_2(\mu\text{-}O)_2(\mu\text{-}O_2CCH_3)](BPh_4)_2 \cdot CH_3CN$, where L is 1,4,7-triazacyclononane. There are no Q-band EPR spectra presented for these $Mn^{III}Mn^{IV}$ complexes. To see if the EPR spectra for $Mn^{III}Mn^{IV}$ complexes have the same broadening effects as seen in the spectra of **1** and **2**, it is important to try other EPR frequencies for the experiments.

Finally, it is quite relevant to note that Khangulov et al.[52] and Fronko et al.[53] have recently reported a variety of EPR signals for the T-catalase from Thermus thermophilus, an enzyme that the 3-Å-resolution X-ray structure[54] shows to have a binuclear Mn site. Treatment of samples of the enzyme with either different exogenous ligands or oxidants or by variation in the temperature gives superpositions of a variety of manganese multiline hyperfine-structured EPR signals. These signals have been attributed to enzymes with either Mn^{II}_2, $Mn^{II}Mn^{III}$, or $Mn^{III}Mn^{IV}$ binuclear sites. Some of these EPR signals do bear some resemblance to those reported in this paper for complexes **1** and **2**.

Acknowledgment. We are grateful for support from NIH Grants HL 13652 (D.N.H.), 1510 RRO 148601A1 (crystallographic instrumentation at Rutgers, H.J.S.), and the Rutgers research council (S.S.I.).

Supplementary Material Available: Tables of experimental and calculated magnetic susceptibility data for complexes **1** and **2**, figure showing fit of data for complex **2**, tables of atomic coordinates and equivalent isotropic thermal parameters for complexes **1** and **2**, tables of H atom parameters and anisotropic thermal parameters for complexes **1** and **2**, and figures showing electrochemistry, 400 MHz ^{1}H NMR, and X-band EPR data for complexes **1** and **2** (22 pages); tables of observed and calculated structure factors for **1** and **2** (66 pages). Ordering information is given on any current masthead page.

(51) Hansson, O.; Aasa, R.; Vanngard, T. *Biophys. J.* **1987**, *51*, 825.

(52) Khangulov, S. V.; Barynin, V. V.; Melik-Adamyan, V. R.; Grebenko, A. I.; Voevodskaya, N. V.; Blumenfeld, L. A.; Dobryakov, S. N.; Il Yasova, B. V. *Bioorg. Khim.* **1986**, *12*, 741-748.

(53) Fronko, R. M.; Penner-Hahn, J. E.; Bender, C. J. *J. Am. Chem. Soc.* **1988**, *110*, 7554-7555.

(54) Barynin, V. V.; Vagin, A. A.; Melik-Adamyuan, V. R.; Grebenko, A. I.; Khangulov, S. V.; Popov, A. N.; Andrianova, M. E.; Vainshtein, B. K. *Sov. Phys. Dokl.* **1986**, *31*, 457-459.

Differential Line Broadening in the NMR Spectrum of Methanol Adsorbed on Sol-Gel Silica

C. J. Hartzell, P. C. Stein, T. J. Lynch,† L. G. Werbelow,*,‡ and William L. Earl*

Contribution from the Los Alamos National Laboratory, Los Alamos, New Mexico 87545.
Received October 3, 1988

Abstract: The nuclear magnetic relaxation characteristics of (^{13}C)methanol adsorbed to sol-gel silica were studied over a wide range of temperatures. The four-line spectra displayed different T_2 values for each line. Inner and outer lines of the quartet displayed different T_1 values. This behavior indicates that temporal correlations between different carbon-proton dipolar interactions are significant. Cross correlations between carbon-proton dipolar couplings and the carbon chemical shift anisotropy are discernible. Adsorbed methanol presents an interesting situation where both even and odd ranks of multispin order are spawned from athermal magnetizations via orientationally dependent spin interactions. These interactions are modulated by highly anisotropic molecular motions.

Various NMR relaxation methodologies provide the chemical researcher with sensitive probes of dynamical structure at the molecular level. Although molecular motions result in the averaging of anisotropic spin couplings, both the nature of the motional averaging process and the magnitude of the anisotropy can be revealed through analysis of the NMR relaxation experiment. Of interest in this work are NMR relaxation studies that probe the creation and subsequent dissipation of multispin order. Temporal correlations between competing orientationally dependent spin interactions generate multispin order in a manner analogous to the generation of multispin order in popularized variants of multipulse NMR.

Although the foundations of multispin NMR relaxation spectroscopy were developed many years ago and are couched in a convenient product operator formalism,[1] only recently has in-

† Department of Chemistry, University of Nevada, Reno, NV 89557.
‡ Department of Chemistry, NMIMT, Socorro, NM 87801.

0002-7863/89/1511-5114$01.50/0

terest in this field started to mature.[2] In particular, the manipulation of relaxation-induced multispin order into easily monitored variants has opened up a new realm of NMR applications.[3]

Sol–gel prepared materials are increasingly of interest to the synthetic inorganic chemist. The sol–gel method involves low-temperature synthesis of inorganic matrices by polymerization of the appropriate monomers. During the last decade, sol–gel processing of metal alkoxides has allowed impressive gains in the control over the physical properties of the resulting metal oxides.[4] In the present study, analysis of correlated NMR relaxation phenomena lends insight into the nature of the adsorption interaction of methanol with silica prepared by the sol–gel process. Recent investigations of methanol adsorption include a ^{13}C NMR study of methanol adsorbed to HY zeolite[5] and studies of deuterated methanol adsorbed to both silica[6] and zeolites.[7] The ^{13}C spectra of methanol on HY zeolite displayed certain spectral features characteristic of multispin order, but the issue was not addressed in that report.

To investigate the motional dependence of the spin relaxation characteristics of (^{13}C)methanol on silica, both longitudinal and transverse magnetization relaxation rates were measured over a wide range of temperatures. Experimental measurements also included determination of various relaxation rates in the rotating frame.

Experimental Section

The silica was prepared by the sol–gel process of hydrolysis and dehydration of tetramethoxysilane (Strem Chemicals). Into 30 mL of ethanol (95%) were added 6.3 mL of tetramethoxysilane, 12 mL of H_2O, and 0.4 mL of glacial acetic acid. The solution was refluxed for 4 h. Solvents were removed from the resulting gel on a rotary evaporator at 60 °C until a powder was formed. The sol–gel silica was then dried at 250 °C for 24 h. The surface area as determined by BET measurements was 302 ± 14 m^2/g. The silica was saturated with (^{13}C)methanol (95% enriched) and then allowed to air dry at ambient temperature for 24 h to give a final loading of 15% by weight.

The relaxation measurements were carried out at temperatures ranging from 190 to 323 K. Longitudinal relaxation was determined by a ^{13}C inversion-recovery experiment, X_{180}–τ–X_{90}–acquire. The recycle delay was 25 s. Transverse relaxation was determined using a X_{90}–τ–Y_{180}–τ echo. The recycle delay was 5 s. The ^{13}C $T^C_{1\rho}$ was determined by varying the ^{13}C spin lock time for the proton-coupled spectra. For these experiments the carbon $\pi/2$ pulse was 3.5–4 μs. The number of scans was 8–16.

Spectra were acquired on a Bruker CXP-200 spectrometer using magic-angle spinning (MAS). The probe was a Doty variable-temperature, MAS probe doubly tuned for ^{13}C (50.3 MHz) and ^1H (200 MHz). Variable temperature was provided by heated or cooled nitrogen gas directed into the probe. A programmable temperature controller maintained the temperature within 0.5 K. Spinning speeds were 2500–3000 Hz.

Relaxation data were analyzed by using a three-parameter least-squares fit of the peak heights to a single exponential. Although the relaxations of the peaks in this study are, in principle, multiexponential, the exponents are too close to permit determination of the different relaxation times. For this reason the measured relaxation times are referred to as "effective" T_1's and T_2's in the discussion below.

The rotating frame relaxation times, T_{CH} and $T_{1\rho}$ were obtained from proton–carbon cross-polarization experiments at 296 K. The relaxation times were determined by curve fitting the peak heights of the proton decoupled spectra as a function of the cross-polarization contact time.

Theory

It can be demonstrated that, for the inversion-recovery experiment as performed, the relative intensities of the four components of the methyl quartet at any time subsequent to the initial perturbation are proportional to the expectation values of the following product operators: $\langle I^C_z(1 - 2S_z + 4S'_z - 8S''_z)\rangle$, $\langle I^C_z(3 - 2S_z - 4S'_z + 24S''_z)\rangle$, $\langle I^C_z(3 + 2S_z - 4S'_z - 24S''_z)\rangle$, $\langle I^C_z(1 + 2S_z + 4S'_z + 8S''_z)\rangle$. If a positive carbon–hydrogen scalar coupling is assumed, these intensities are associated with the specific spectral components from low field to high field, respectively. In this expression, I is a single spin operator and the S's are composite spin operators defined as follows:

$$S_z = I^H{}_z + I^{H'}{}_z + I^{H''}{}_z$$

$$S'_z = I^H{}_z I^{H'}{}_z + I^{H'}{}_z I^{H''}{}_z + I^H{}_z I^{H''}{}_z$$

$$S''_z = I^H{}_z I^{H'}{}_z I^{H''}{}_z$$

At thermal equilibrium, in the high-temperature limit, all multispin order is negligible in comparison to one spin order. In this limit, the relative intensities of the four members of the quartet appear in the familiar ratio 1:3:3:1. Conversely, during the course of relaxation, any deviation from the 1:3:3:1 intensity ratio is evidence (by definition) that multispin order has been created via dissipative processes. Note that the summed intensity of the outermost components reflects only odd spin order, whereas the differential intensity of the outermost lines is described by even spin order. A similar realization obtains for the two central components. The summed intensity of all four lines is proportional to $\langle I^C_z\rangle$. Pure two-spin order, three-spin order, or four-spin order can be associated with weighted combinations of multiplet intensities. Of interest in this work is the three-spin order term $\langle I^C_z S'_z\rangle$, which is proportional to 3 times the outer lines minus the central lines.

Implicitly, it follows that each of the four single quantum transition operators involving I^C_+ can be identified with a unique product operator: $I^C_+(1 - 2S_z + 4S'_z - 8S''_z)$, $I^C_+(3 - 2S_z - 4S'_z + 24S''_z)$, $I^C_+(3 + 2S_z - 4S'_z - 24S''_z)$, or $I^C_+(1 + 2S_z + 4S'_z + 8S''_z)$. When all multispin order is absent, the four members of this quartet are characterized by equal line width factors. If only three-spin order is generated through relaxation, the line-width factor of the outermost components differs from the central components. If two-spin order is generated, the line widths of the two upfield components differ from their downfield complements. Proper recognition of these predicted anomalous line-width variations in methyl group relaxation studies provides a simple means for evaluating the relative importance of various time-dependent interactions and the degree of correlation between these interactions. Since multispin order can be created through relaxation effects other than cross correlation,[8] a certain degree of caution must be exercised.

(1) Werbelow, L. G.; Grant, D. M. *Adv. Magn. Reson.* **1977**, *9*, 189.
(2) Exemplary recent studies include: (a) Chenon, M. T.; Bernassau, J. M.; Coupry, C. *Mol. Phys.* **1985**, *54*, 277. (b) Brown, M.; Grant, D. M.; Horton, W. J.; Mayne, C. L.; Evans, G. T. *J. Am. Chem. Soc.* **1985**, *107*, 6698. (c) Farrar, T. C.; Quintero-Arcaya, R. A. *Chem. Phys. Lett.* **1985**, *122*, 41. (d) Withers, S.; Madsen, N.; Sykes, B. *J. Magn. Reson.* **1985**, *61*, 545. (e) Konigsberger, E.; Sterek, H. *J. Chem. Phys.* **1985**, *83*, 2723. (f) Farrar, T. C.; Adams, B. R.; Grey, G. C.; Quintero-Arcaya, R. A.; Zuo, Q. *J. Am. Chem. Soc.* **1986**, *108*, 8190. (g) Sterk, H.; Konigsberger, E. *J. Phys. Chem.* **1986**, *90*, 916. (h) Ayant, Y.; Kernevez, N.; Thevand, A.; Werbelow, L. G.; Culcasi, M.; Gronchi, G.; Tordo, P. *J. Magn. Reson.* **1986**, *70*, 446. (i) Ayant, Y.; Thevand, A.; Werbelow, L. G.; Tordo, P. *J. Magn. Reson.* **1986**, *72*, 251. (j) Heatley, F. *J. Chem. Soc., Faraday Trans. 1* **1987**, *83*, 2593. (k) Farrar, T. C.; Locke, I. C. *J. Chem. Phys.* **1987**, *87*, 3281. (l) Farrar, T. C.; Quintero-Arcaya, R. A. *J. Phys. Chem.* **1987**, *91*, 3224. (m) Brondeau, J.; Canet, D.; Millot, H.; Nery, H.; Werbelow, L. G. *J. Chem. Phys.* **1985**, *82*, 2212. (n) Anet, F. A. L. *J. Am. Chem. Soc.* **1986**, *108*, 7102. (o) Hastlinger, E.; Kalchauser, H.; Robien, W. *J. Mol. Liquids* **1984**, *28*, 223. (p) Gueron, M.; Leroy, J. L.; Griffey, R. H. *J. Am. Chem. Soc.* **1984**, *106*, 7262. (q) Brown, M. S.; Mayne, C. L.; Grant, D. M.; Chou, T. C.; Allred, E. L. *J. Phys. Chem.* **1984**, *88*, 2708. (r) Voight, J.; Jacobsen, J. *J. Chem. Phys.* **1983**, *78*, 1693. (s) Fuson, M. M.; Prestegard, J. H. *Biochemistry* **1983**, *22*, 1311. (t) Bendall, M. R.; Pegg, D. T. *J. Magn. Reson.* **1983**, *53*, 40.
(3) Exemplary studies include: (a) Muller, N.; Bodenhausen, G.; Ernst, R. R. *J. Magn. Reson.* **1985**, *65*, 531. (b) Rance, M.; Wright, P. E. *Chem. Phys. Lett.* **1986**, *124*, 572. (c) Muller, N. *Chem. Phys. Lett.* **1986**, *131*, 218. (d) Keeler. J.; Sanchez-Ferrando, F. *J. Magn. Reson.* **1987**, *75*, 96. (e) Kay, L. E.; Prestegard, J. H. *J. Am. Chem. Soc.* **1987**, *109*, 3829. (f) Muller, N.; Bodenhausen, G.; Ernst, R. *J. Magn. Reson.* **1987**, *75*, 297. (g) Jaccard, G.; Wimperis, S.; Bodenhausen, G. *Chem. Phys. Lett.* **1987**, *138*, 601. (h) Wimperis, S.; Bodenhausen, G. *Chem. Phys. Lett.* **1987**, *140*, 41. (i) Bull, T. E. *J. Magn. Reson.* **1987**, *72*, 397. (j) Bohlen, J. M.; Wimperis, S.; Bodenhausen, G. *J. Magn. Reson.* **1988**, *77*, 589. (k) Dalvit, C.; Bodenhausen, G. *J. Am. Chem. Soc.*, submitted.
(4) Turner, C. W.; Franklin, K. J. In *Science of Ceramic Chemical Processing*; Hench, L. L., Ulrich, D. R., Eds.; Wiley: New York; 1986; p 81.
(5) Bronnimann, C. E.; Maciel, G. E. *J. Am. Chem. Soc.* **1986**, *108*, 7154.
(6) Seymour, S. J.; Cruz, M. I.; Fripiat, J. J. *J. Phys. Chem.* **1973**, *77*, 2847.
(7) Eckman, R. R.; Vega, A. J. *J. Phys. Chem.* **1986**, *90*, 4679.
(8) For example: Werbelow, L. G.; Pouzard, G. *J. Phys. Chem.* **1981**, *85*, 3887.

The quantitative transformation of athermal one-spin order into transient multispin order is described by a kinetic master equation of the form[1]

$$-\mathrm{d}\nu_i(t)/\mathrm{d}t = \sum_j \Gamma_{ij}\nu_j(t) \tag{1}$$

The various "magnetization modes", ν_i, are identified with linearly independent manifestations of spin order, and the elements of the kinetic transport matrix, Γ_{ij}, are given by various nonlinear combinations of specific rate constants. In the appropriate limits, these rate constants can be evaluated quite simply.[9]

Expressions that describe the relaxation characteristics of the longitudinal magnetizations for the $^{13}CH_3$ spin grouping have been derived previously.[10] It follows that the four measurable, diagonal product operators couple together along with seven, unobservable magnetizations. Obviously, the detailed expressions defining the time evolution of any form of spin order are exceedingly complex. In the absence of spacial isotropy, the dimensionality of this coupling increases to 15.[11] The short-time behavior of the various longitudinal magnetization modes, subsequent to a semiselective π-pulse perturbation of the ^{13}C quartet, can be described as follows:

$$\frac{\mathrm{d}\langle I^C_z S_z(t\rightarrow 0)\rangle}{\mathrm{d}t} \propto J_{\mathrm{CSA\cdot D}}(\omega_C) = \frac{2\pi}{5}(\omega_C\Delta\sigma) \times \left(\frac{\gamma_C\gamma_H\hbar}{r_{CH}^3}\right)\int_0^\infty \langle Y^0_2(\Omega_{CSA}(t))\ Y^0_2(\Omega_{CH}(0))\rangle \exp(-i\omega_C t)\ \mathrm{d}t$$

$$\frac{\mathrm{d}\langle I^C_z S'_z(t\rightarrow 0)\rangle}{\mathrm{d}t} \propto J_{HCH}(\omega_C) = \frac{6\pi}{5}\left(\frac{\gamma_C\gamma_H\hbar}{r_{CH}^3}\right)^2\int_0^\infty \langle Y^0_2(\Omega_{CH}(t))\ Y^0_2(\Omega_{CH'}(0))\rangle \exp(-i\omega_C t)\ \mathrm{d}t$$

$$\frac{\mathrm{d}\langle I^C_z S''_z(t\rightarrow 0)\rangle}{\mathrm{d}t} \sim 0 \tag{2}$$

The term $J_{\mathrm{CSA\cdot D}}(\omega_C)$ defines the spectral representation of the temporal cross correlation, sampled at the carbon Larmor frequency, between a carbon–proton dipolar (D) interaction and the carbon chemical shift anisotropy (CSA). Similarly, the term $J_{HCH}(\omega_C)$ defines the cross-correlated spectral density associated with two distinct carbon–proton dipolar interactions. These two cross-correlated spectral densities depend upon various interaction constants such as nuclear magnetogyric ratios, γ, C–H internuclear distances, r_{CH}, and the methyl carbon shift anisotropy, $\Delta\sigma$. The dynamical information is embodied in the reduced spherical harmonic correlation function, $\langle Y^0_2(\Omega_i(t))\ Y^0_2(\Omega_j(0))\rangle$. The polar angles, Ω_i, position the principal axis of the ith interaction tensor. Additional clarification of notation and meaning of cross correlation is in the literature.[1,12] In the experiments performed, four-spin order is generated only through indirect couplings. This is a consequence of the fact that the various spin interactions of importance in NMR are, at most, bilinear or quadratic in angular momentum operators.

Exacting treatments of the single quantum transverse magnetizations are uniquely complicated. The CSA interaction, unlike any other interaction encountered in NMR, cannot be written as a scalar contraction of irreducible spherical tensors, and hence the longitudinal and transverse relaxation rates need not be related. However, the outer lines of the ^{13}C quartet are simple lines characterized by a unique Lorentzian width.[13] If carbon nuclear magnetic relaxation is affected by carbon–proton dipolar and carbon CSA interactions, the half-width (s^{-1}) of the high-field $(1/T_2)_+$ and low-field $(1/T_2)_-$ components (assuming a positive C–H scalar coupling constant) are defined as follows:

$$(1/T_2)_\pm = [{}^8/_3 J_{CSA}(0) + 2J_{CH}(0) + 4J_{HCH}(0) \mp 8J_{CSA\cdot D}(0)] + [2J_{CSA}(\omega_C) + {}^3/_2 J_{CH}(\omega_C) + {}^3/_2 J_{HCH}(\omega_C) \mp 6J_{CSA\cdot D}(\omega_C)] + [{}^1/_2 J_{CH}(\omega_H - \omega_C) + {}^3/_2 J_{CH}(\omega_H) + 3J_{CH}(\omega_H + \omega_C)] + [3J_{HH}(\omega_H) + 3J_{HHH}(\omega_H) + 6J_{HH}(2\omega_H)] \tag{3}$$

The spectral densities, J_{CSA} and $J_{CH}(J_{HH})$ are the carbon CSA and carbon–hydrogen (hydrogen–hydrogen) autocorrelated spectral densities. Other relaxation contributions add equally to each of these two spectral components. The differential width between the outermost components, $(1/T_2)_- - (1/T_2)_+$, depends only upon cross-correlated spectral densities and equals $16J_{\mathrm{CSA\cdot D}}(0) + 12J_{\mathrm{CSA\cdot D}}(\omega_C)$. Each central component is described as a superposition of three Lorentzians. However, in the absence of dipolar–CSA temporal correlation, the central components are identical in both width and shape, and yet the central components will differ in width and shape from the outer components.

It is important to mention that, in general, the values of T_2 determined by spin–echo techniques are sensitive to the time interval between the refocusing pulse and echo formation. Only when this interval is long compared to $(2\pi J)^{-1}$ does one measure the T_2 defined in eq 3.[14] However, the adiabatic width, which is dominant in the present study, does not depend on this time interval.

It is instructive to note that even the simple one-pulse sequence, $(\pi/2)_C$–detect, probes multispin order and can be used to correlate various spin interactions. In the present case, the observation of two-spin order is indicated by differential broadening of higher field components compared to the symmetrically positioned, spin-inverted, downfield counterparts, whereas differential broadening between inner and outer components corresponds to three-spin order. Continuing this line of argument, it should be recognized that the rudimentary informational content of the simplest magnetic relaxation study encodes the correlative powder of higher profile, two-dimensional NMR spectroscopies.

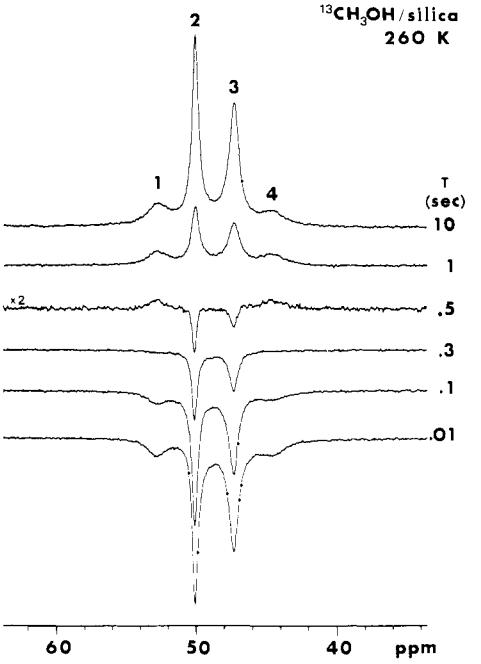

Figure 1. Spectra of the inversion-recovery experiment for (^{13}C)methanol adsorbed to silica at 260 K. The 0.5-s spectrum is multiplied by 2 to emphasize the difference in the recovery of the inner and outer lines.

Results and Discussion

To investigate the differential line broadening that was observed in the NMR spectrum of (^{13}C)methanol adsorbed to sol–gel silica,

(9) Redfield, A. G. *NMR: Basic Princ. Prog.* **1976**, *13*, 1.
(10) (a) Werbelow, L. G.; Grant, D. M. *J. Chem. Phys.* **1975**, *63*, 544. (b) Bain, A. D.; Lynden-Bell, R. M. *Mol. Phys.* **1975**, *30*, 325.
(11) Werbelow, L. G.; Grant, D. M.; Black, E. P.; Courtieu, J. M. *J. Chem. Phys.* **1978**, *69*, 2407.
(12) Werbelow, L. G.; Grant, D. M. *J. Magn. Reson.* **1975**, *20*, 554.
(13) Hoffman, R. A. *Adv. Magn. Reson.* **1970**, *4*, 87.
(14) Vold, R. R.; Vold, R. L. *J. Chem. Phys.* **1976**, *64*, 320.

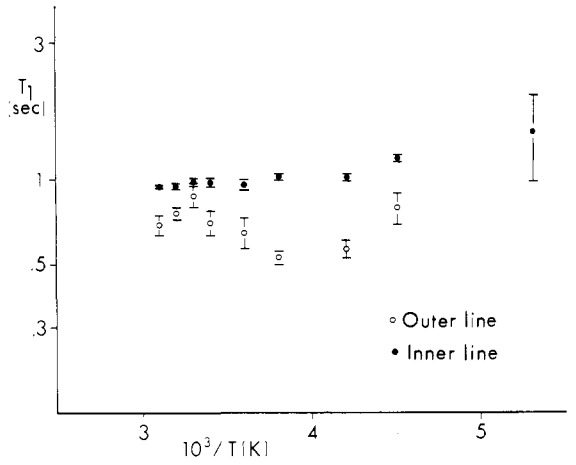

Figure 2. Plot of the effective T_1 vs $1000/T$ for $^{13}CH_3OH$/silica. Values for the downfield outer and inner lines are shown (lines 1 and 2, respectively). At 190 K the outer lines are not distinguishable due to the line width.

Table I. T_2[b,c] Values for the Four Lines of the (^{13}C)Methanol/Silica Spectrum

	line			
temp[a]	1	2	3	4
323	3.1	12.7	8.0	2.6
314	5.1	14.9	8.9	2.0
296	3.0	10.1	5.9	1.7
275	2.2	9.2	5.7	1.9
260	2.1	7.2	4.3	1.7
240	1.9	4.3	2.7	1.5
220	1.0	1.9	1.4	1.0
190		.21		

[a] Temperature in kelvin. [b] T_2 values in milliseconds. [c] Errors are ±0.3 ms.

T_1 and T_2 studies were performed over the temperature range 190–323 K. The spectra from the inversion-recovery experiment at 260 K are shown in Figure 1. The four lines of the equilibrium spectrum (τ = 10 s) do not reveal the normal 1:3:3:1 peak height ratios characteristic of an AX_3 spin system. However, the peaks integrate to the expected 1:3:3:1 intensity ratios. The difference in peak heights can be attributed to a difference in line widths for the four peaks. In a liquid methanol spectrum recorded at the same field strength the line widths apparently are equal for all four components. It should be noted that T_1 studies of liquid methanol have revealed asymmetric multiplet relaxation.[15]

In the inversion-recovery experiments, the inner and outer lines passed through a null at different times. In Figure 1, this is particularly obvious in the τ = 0.5 s spectrum. Lines 1 and 4 have passed through the null point, while lines 2 and 3 have not yet nulled. The effective T_1 values (see Experimental Section) for the four lines of the 260 K spectrum are 0.53, 0.96, 0.93, and 0.46 ± 0.03 s (lines 1–4, respectively). In Figure 2, the effective T_1 values determined at various temperatures are plotted. Only the values for lines 1 and 2 are shown. These are referred to as the outer and inner lines, respectively. It is clear from this plot that the effective T_1 values of the outer and inner lines differ throughout the temperature range studied. The values for lines 3 and 4 are not shown since they differ very little from lines 2 and 1, respectively. The T_1 values exhibit little change over the temperature range studied. This may indicate that motions capable of causing relaxation (in the tens of megahertz to gigahertz range) have a low activation energy. This would be expected for a methyl group rotation.

The results of the T_2 studies at variable temperature are plotted in Figure 3. Again, only lines 1 and 2 are plotted. Table I presents the effective T_2 values for the four lines at all temperatures studied. The effective T_2 values for lines 2 and 3 display a ratio

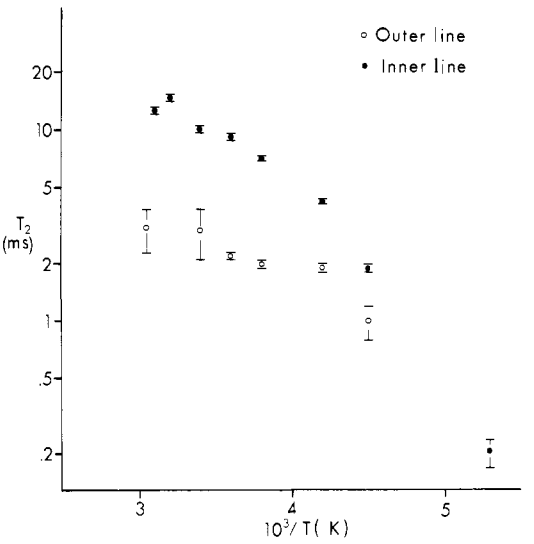

Figure 3. Plot of effective T_2 vs $1000/T$ for the outer and inner lines (lines 1 and 2) of (^{13}C)methanol/silica.

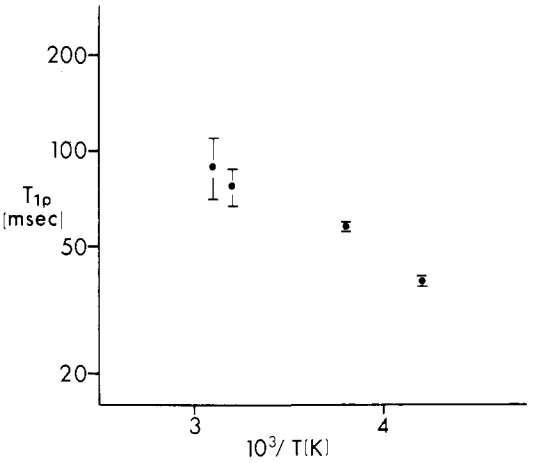

Figure 4. Plot of ^{13}C $T^C_{1\rho}$ determined at selected temperatures. Values are shown for line 2 only.

of line 3 to line 2 of 0.6 ± 0.02 at all temperatures. The effective T_2 values for the spectrum in Figure 1 are 2.1, 7.2, 4.3, and 1.7 ± 0.3 ms. As stated above, the difference in the T_2 values of lines 1 and 4 or lines 2 and 3 reflects two-spin order while the difference in lines 1 and 2 or lines 3 and 4 (inner and outer lines) reflects three-spin order.

Results of ^{13}C $T^C_{1\rho}$ measurements at selected temperatures are plotted in Figure 4. A decrease in $T^C_{1\rho}$ is observed over the four temperatures plotted. The slope predicts a motional activation energy of 6.5 kJ/mol. The absence of a minimum in this temperature range indicates that motions in the region of 100 kHz are absent.

The cross-polarization spectra of (^{13}C)methanol on silica were characterized by a continuous increase in spectral intensity with an increase in contact time to an optimum contact time of 15 ms. At contact times exceeding 20 ms the spectral intensity decreased. This contact time is slightly longer than the values of 2–5 ms seen in organic solids. However, the behavior is unlike the oscillatory response of intensity to change in contact time which is characteristic of J cross polarization observed in liquids.[16]

From variable contact time studies it was determined that the cross-relaxation time in the rotating frame, T_{CH}, was 4 ± 0.5 ms and the proton relaxation time from spin lock, $T_{1\rho}$, was 50 ± 3 ms. That this $T_{1\rho}$ measures proton rather than carbon relaxation from spin lock is verified by noting that the ^{13}C $T^C_{1\rho}$ value in

(15) Daragan, V. A. *Dokl. Akad. Nauk SSR* **1977**, *232*, 114.

(16) Bertrand, R. D.; Moniz, W. B.; Garroway, A. N.; Chingas, G. C. *J. Am. Chem. Soc.* **1978**, *100*, 5227.

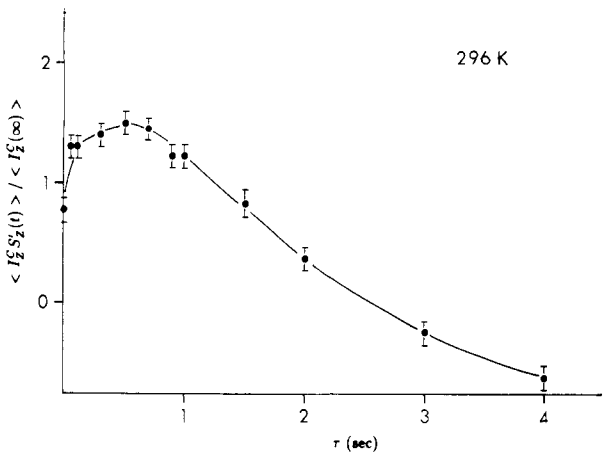

Figure 5. Plot of $\langle I^C_z S'_z(t)\rangle / \langle I^C_z(\infty)\rangle$ (3 times the outer lines minus the inner lines) taken from the inversion-recovery experiment at 296 K. The values are determined from the integrated line intensities.

Figure 4 is nearly twice this value at 296 K. The proton $T_{1\rho}$ of 50 ms is slightly lower than the range of values (60–110 ms) determined by Sindorf and Maciel[17] for the protons on silica gels heated under vacuum at temperatures exceeding 100 °C. These comparisons indicate that the surface of the sol–gel preparation in this study contains hydroxyl moieties. In fact, silica preparations heated to 250 °C still contain a high proportion of silanol groups which only dehydrate to bridging oxygens above 400 °C.[17]

Proton T_1 and T_2 values were determined at 296 K. The T_2 values for the two doublet components were 3.0 and 2.6 ± 0.3 ms. These values agree with the value obtained for methanol on an aluminosilicate catalyst at a coverage of 2.5 monolayers.[18] The T_1 values obtained were 0.85 and 0.94 ± 0.04 s. These values for T_1 are larger than the range observed by Sindorf and Maciel of 60–400 ms. These authors reported that T_1's were much less sensitive to surface hydration than were the $T_{1\rho}$'s.

As discussed in the Theory section, three-spin order is associated with a weighted combination of line intensities, specifically, 3 times the outer lines minus the inner lines. This combination is proportional to $\langle I^C_z S'_z\rangle$. In Figure 5, the values $\langle I^C_z S'_z(t)\rangle / \langle I^C_z(\infty)\rangle$ determined from the inversion-recovery experiment performed at 296 K are plotted as a function of the variable delay, τ. This calculation utilizes the integrated intensities. In the absence of multispin order, such a plot would give a straight line. Similar plots of all temperature studies fell within the error limits of the curve shown. This implies that the motion did not change significantly over this temperature range.

To analyze the source of the variation in T_1 across the spectrum, we refer to the theory outlined in the preceding section. Applying this to the data shown above, it is recognized that there are vestiges of relaxation-induced two- and three-spin order present in these studies. Since the most marked multiplet relaxation asymmetries occur between the pair of inner peaks and the pair of outer peaks (i.e., three-spin order dominantes two-spin order), one concludes that dipolar–dipolar cross correlations prevail over dipolar–CSA cross correlations. There are two possible explanations for this observation: either the intrinsic dipolar–dipolar cross correlations are stronger than the dipolar–CSA cross correlations or the CSA interaction constant ($\omega_C \Delta\sigma$) is much weaker than the dipolar interaction constant ($\gamma_C \gamma_H \hbar r_{CH}^{-3}$).

This issue is resolved by noting that during the inversion-recovery experiment, the outer lines recover more quickly than the central lines (refer to Figure 5). Assume a reorientational model in which reorientations about the methyl triad axis are characterized by a rotational diffusion constant $D_\parallel$ and reorientations of this axis are characterized by a rotational diffusion constant $D_\perp$. It can be shown that if $D_\parallel/D_\perp$ is less than $(13 + (513)^{1/2})/4 \sim 9$, then J_{HCH} is negative.[19] Only for very large motional anisotropies does the normalized dipolar–dipolar cross correlation

$$\frac{J_{HCH}(0)}{J_{CH}(0)} = \frac{\int_0^\infty \langle Y^0_2(\Omega_{CH}(t))\ Y^0_2(\Omega_{CH'}(0))\rangle\ dt}{\int_0^\infty \langle Y^0_2(\Omega_{CH}(t))\ Y^0_2(\Omega_{CH}(0))\rangle\ dt}$$

become appreciably positive.[14,20] By comparison to theoretical plots presented in ref 10a, it is apparent that $D_\parallel/D_\perp \gg 1$ for the system being studied.

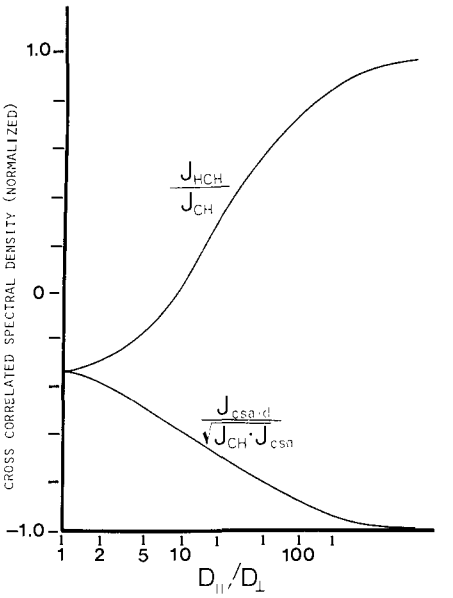

Figure 6. Plot of the normalized cross-correlations $J_{CSA\cdot D}$ and J_{HCH} as a function of motional anisotropy.

In this same motional limit, the dipolar–CSA interactions are anticorrelated. The basis for this prediction is summarized by Figure 6, which plots the cross correlations, $J_{CSA\cdot D}$ and J_{CH} (normalized such that the interaction constants are suppressed) as a function of motional anisotropy. Equation 3 indicates that if the dipolar–CSA cross correlation is negative and the C–H scalar coupling is positive, the higher field component will be broadened relative to the lower field component. This is in agreement with the experimental result. Conversely, once the sign of the dipolar–CSA cross correlation is deduced, the absolute sign of the carbon–hydrogen scalar coupling constant can be determined.

It is important to recognize that model-independent descriptions of the cross-correlation function would lead to these same conclusions;[21] hence the foregoing argument is not dependent upon the validity of a rotational diffusion model. Furthermore, one should be cognizant of a common but mistaken belief that normalized cross-correlation factors in magnetic relaxation are limited to the half-range, 0 to 1, or the range spanned by the second-rank Legendre polynominal, $-1/2$ to $+1$. In the present case, rapid reorientation effectively projects all anisotropic spin interactions onto a common axis. Hence, all interactions are rendered dynamically equivalent and, depending upon the signed magnitude of this projection, $(3\cos^2\theta - 1)/2$, are either wholly correlated or anticorrelated. The interaction strengths of the correlated interactions may differ significantly.

Note, also, that dipolar–CSA cross correlations appear significant for T_2 studies but are relatively unimportant for the T_1 studies. This behavior is predicted and is traced to the fact that zero-frequency spectral densities are dominant. Nonsecular line-width contributions are effectively quenched. Hence, various interference terms assume greater prominence (cf. eq 1 and

(17) Sindorf, D. W.; Maciel, G. E. *J. Am. Chem. Soc.* **1983**, *105*, 1487.
(18) Panchenkov, G. M.; Erchenkov, V. V.; Danchev, M. D. *Russ. J. Phys. Chem.* **1973**, *47*, 1623.
(19) (a) Hubbard, P. S. *J. Chem. Phys.* **1970**, *52*, 563. (b) Werbelow, L. G.; Grant, D. M. *J. Magn. Reson.* **1975**, *21*, 369.
(20) Werbelow, L. G.; Grant, D. M. *Can. J. Chem.* **1977**, *55*, 1558.
(21) (a) Hubbard, P. S. *Phys. Rev.* **1969**, *180*, 319. (b) Lipari, G.; Szabo, A. *J. Am. Chem. Soc.* **1982**, *104*, 4546.

discussions in ref 2f and 12). In the limit where zero-frequency terms dominate and motions are highly anisotropic, if $J_{CH}(0) \sim {}^4/_9 J_{CSA}(0)$ (i.e., $\gamma_C\gamma_H\hbar r_{CH}^{-3} \sim {}^2/_3\omega_C\Delta\sigma$), then $(1/T_2)_+/(1/T_2)_- \sim \infty$. In the present case, $(1/T_2)_+/(1/T_2)_- \sim 1.4 \pm 0.2$, indicating $\gamma_C\gamma_H\hbar r_{CH}^{-3} \sim 8\omega_C\Delta\sigma$. Therefore, the approximate magnitude of the methyl carbon CSA is 60 ± 20 ppm. Since nonsecular terms may not be entirely negligible, this value for $\Delta\sigma$ should be considered as a lower limit. Liquid-crystalline and solid-state studies yield values in the range 65 ± 15 ppm.[22]

In the limit where $J_{CH} = J_{HCH}$ and adiabatic terms dominate, the central two lines of the methyl quartet are Lorentzian with

$$\left(\frac{1}{T_2}\right)_{\pm}^{\text{inner}} = {}^8/_3 J_{CSA}(0) + {}^2/_3 J_{CH}(0) \mp {}^8/_3 J_{CSA\cdot D}(0)$$

Although this limit does not strictly obtain, it is apparent from Figure 1 that the central lines are narrowed relative to the outer lines because of the diminished importance of carbon–hydrogen dipolar interactions. Furthermore, the differential broadening between the two central components is more pronounced than the differential broadening between the two outer components, once again in agreement with theory.

It is remarkable that dipolar–CSA cross correlations are clearly important even though $J_{CH}(0) \sim 60 J_{CSA}(0)$. It has been noted elsewhere[23] that utilization of relaxation-induced multispin order may make it possible to observe anisotropic spin interactions that are intrinsically 3 or 4 orders of magnitude weaker than a dominant, temporally correlated interaction. This realization has exciting implications and awaits exploitation.

Conclusions

This relaxation study indicates that the magnetic relaxation behavior of adsorbed methanol is dominated by highly anisotropic motions. At least one characteristic motion is long on a time scale compared with $1/\omega_C$, whereas another motion (presumably rotation about the $-CH_3$ axis) is short compared to $1/\omega_C$. This is consistent with a model of methanol that is hydrogen bonded to either siloxane or free silanol. The silanol functionality has been shown[17] to predominate in silicas treated at 250 °C. The presence of these hydroxyl groups is consistent with the proton relaxation data presented above. Future studies will investigate the effects of higher temperature treatment of the sol–gel silica on the relaxation behavior of adsorbed methanol.

Studies[24] in this laboratory have shown that at lower methanol loading, cross-polarization spectra reveal a broad and narrow component with different T_1 and T_{CH} values. At the loading levels of the current experiment the broad spectral component is not evident. The implication, however, is that there exists at low abundance at least one methanol species that experiences a strong proton dipole-coupling.

The argument has been made that interference or cross-correlation effects such as those described in this work provide a detailed description of molecular dynamics and anisotropic interaction at the molecular level. The relative magnitudes of dipolar and CSA interactions as well as the degree of dipolar–dipolar and dipolar–CSA cross correlation have been determined from relatively straightforward relaxation studies performed at a single field strength. Cross correlations and the manifestation of cross-correlation multispin order can be used to determine absolute signs of various spin couplings and position the principal axes of spin interaction. Most importantly, the evolution of multispin order is extremely sensitive to motional anisotropies and can be used to investigate highly anisotropic systems where conventional NMR relaxation studies would fail.

The studies and analyses described in this work do not exhaust the informational content of temporal correlation of anisotropic spin interaction. Experiments in progress include (i) the use of complementary pulse perturbations that selectively explore additional cross-correlation factors, (ii) studies involving the selective creation and dissipation of four-spin order, and (iii) the application of multiquantum relaxation that probes alternative manifestations of multispin order and cross correlation. It is anticipated that dynamic correlation NMR spectroscopy will become the method of choice in the study of dynamic structure.

Acknowledgment. We acknowledge Los Alamos National Laboratory Director's Funded Postdoctoral Fellowships for support of C.J.H. and P.C.S. This work was supported by the U.S. Department of Energy under Contract No. W-7405 ENG-86.

Registry No. Methanol-^{13}C, 14742-26-8.

(22) (a) Pines, A.; Gibby, M.; Waugh, J. S. *Chem. Phys. Lett.* **1972**, *15*, 373. (b) Strub, H.; Beeler, A. J.; Grant, D. M.; Michl, J.; Cutts, P. W.; Zilm, K. W. *J. Am. Chem. Soc.* **1983**, *105*, 3333.

(23) Werbelow, L. G.; Allouche, A.; Pouzard, G. *J. Chem. Soc., Faraday Trans. 2* **1987**, *83*, 871.

(24) Hartzell, C. J.; Lynch, T. J.; Earl, W. E., unpublished work.

Study of ^{31}P NMR Chemical Shift Tensors and Their Correlation to Molecular Structure

Sun Un[†,‡] and Melvin P. Klein*[,‡]

Contribution from the Department of Chemistry and Chemical Biodynamics Division, Lawrence Berkeley Laboratory, University of California, Berkeley, Berkeley, California 94720.
Received October 13, 1988

Abstract: The nature of the ^{31}P anisotropic chemical shift interaction is examined by using magic-angle sample spinning NMR. Linear correlations between the principal values of the ^{31}P chemical shift tensor, P–O bond lengths, and O–P–O bond angles are established. On the basis of a previously established correlation between P–O bond length and d_P–p_O π-bond order, values of the ^{31}P chemical shift tensor elements were determined to be linearly related to d_P–p_O π-bond order. Furthermore, from correlations between bond lengths and bond angles, it was concluded that for the phosphates reported in this study the π- and σ-bond contributions to the ^{31}P chemical shift interaction are not independent of each other and, hence, cannot be separated into distinct terms. A review of other phosphoryl derivatives suggests that these observations may be general for other quadruply coordinated phosphorus compounds.

More than 20 years ago, Lechter and Van Wazer[1] identified three factors that determined the changes in ^{31}P isotropic chemical shifts. The equation

$$\Delta\delta = a\Delta n_\pi - b\Delta\chi + c\Delta\theta_\sigma \quad (1)$$

compactly summarizes their findings, where a, b, and c are con-

[†] Department of Chemistry.
[‡] Chemical Biodynamics Division.

0002-7863/89/1511-5119$01.50/0